Geosciences and Engineering, Vol. 14, No. 1 (2026), pp. 43–60.
https://doi.org/10.33030/geosciences.2026.01.004

PETROPHYSICAL RESPONSE OF SANDSTONE AND TUFF TO WATER AND FREEZE–THAW

RAMI MOGHRABI [1]*, ÁKOS TÖRÖK [2], BALÁZS VÁSÁRHELYI[3]
[1]**Budapest University of Technology and Economics (BME), Hungary;*
ramifadimoghrabi@edu.bme.hu
[2]*Department of Geotechnical and Geological Engineering, BME, Hungary;*
torok.akos@emk.bme.hu
[3]*Geotechnical and Geology Engineering department, BME, Hungary;*
vasarhelyi.balazs@emk.bme.hu
[1]*https://orcid.org/0009-0005-1046-3791*
[2]*https://orcid.org/0000-0002-5394-4510*

Abstract: This study evaluates the durability of 11 Hungarian lithotypes (sandstone and volcanic tuff) from the Eger region under water saturation and 100 freeze–thaw (F–T) cycles. Utilizing 468 specimens, physical degradation was quantified via ultrasonic wave velocities and dynamic moduli. Results indicate that while saturation initially increases P-wave velocity through pore-filling, cyclic freezing induces progressive microstructural attenuation, primarily within the first 50 cycles. Tuff varieties exhibited high frost sensitivity and significant stiffness loss due to high open porosity and zeolitic alteration. Conversely, sandstone maintained superior structural integrity. Strong correlations between acoustic parameters and elastic moduli confirm that non-destructive testing effectively characterizes stone durability.

Keywords: *tuff, sandstone, ultrasonic wave velocity, dynamic elastic moduli, freeze–thaw cycles, low-temperature deterioration*

1. INTRODUCTION

Sandstone and tuff are widely used natural stones with contrasting origins and responses to environmental stress. Sandstone forms from the compaction and cementation of detrital materials such as quartz, feldspar, and lithic fragments, where intergranular pores control permeability and mechanical behavior. In contrast, tuff is a pyroclastic rock composed of volcanic ash and rock fragments whose rapid deposition often results in a highly porous, weakly bonded structure. These mineralogical and textural differences lead to distinct responses under water infiltration, freeze–thaw (F-T) cycles, and thermal fluctuations, which progressively affect density, stiffness, and long-term durability.

Previous studies have shown that environmental factors, including temperature variations and water saturation, can significantly influence the physical and mechanical behavior of sedimentary rocks (Moghrabi et al. 2025a). Weathering factors such as precipitation, humidity variations, ice crystallization, and salt

accumulation play a critical role in determining the long-term durability of natural building stones. Among these, the interaction between moisture and porosity is particularly influential. The internal pore network of rocks, which can range from less than 5 % to more than 50 % by volume, governs fluid transport, air exchange, and the overall mechanical response of the material. High porosity facilitates the capillary rise and retention of water, creating conditions favorable for physical stress. Studies have shown that the size, shape, and connectivity of pores directly control moisture migration and evaporation rates, thereby influencing the onset of internal stresses and crack propagation (Putnis and Mauthe 2000; Ruedrich et al. 2011). When saline or polluted water enters the pores, crystallization pressure builds up during drying and freezing, gradually widening the pore throats and reducing cohesion (Scherer 2004; Rodriguez-Navarro and Doehne 1999). Siegesmund et al. (2023) observed that the presence of ice lenses inside the pore spaces accelerates deterioration, leading to a complex interplay between mechanical fatigue and mineral dissolution.

Numerous studies have identified strong correlations between P-wave velocity (V_p), density, S-wave velocity (V_s), dynamic Young's modulus (E_{dyn}), dynamic Shear modulus (G_{dyn}), dynamic Bulk modulus (K_{dyn}), and dynamic Poisson's ratio (υ_{dyn}), making these parameters reliable indicators of internal damage (Altındag 2012; Arman et al. 2020; Kahraman 2001). As environmental exposure alters the pore framework, the reduction in wave velocity directly reflects the progressive degradation of stiffness and cohesion.

Repeated F–T cycles increase porosity as water-to-ice transitions generate frost-heaving pressures (Jia et al. 2020; Zhang et al. 2025). Initial cycles promote pore expansion and interconnection, particularly in highly porous volcanic tuffs, which absorb more water than sandstone and accelerate deterioration. This microstructural damage is evidenced by decreased longitudinal wave velocities (V_p) and density; Jia et al. (2020) identified a strong negative correlation between V_p and F–T damage. Consequently, both velocity and elastic moduli decline as freezing intensifies (Ma et al. 2023; Niu et al. 2024; Zhou et al. 2025).

The susceptibility of natural stones to environmental stressors varies significantly across global climate zones. Regions with mild-temperate climates, such as Southern Italy (Naples) or parts of the Philippines, subject lithotypes to average annual temperatures of 22–25 °C (MeteoNapoli 2023; PAGASA 2023). In humid tropical and coastal regions, such as Metro Manila, stones like the Guadalupe tuff or the Campanian ignimbrite (Neapolitan yellow tuff) undergo prolonged wetting (de Gennaro et al. 2000; Galaura et al. 2019). Conversely, temperate and continental climates in Central and Northern Europe experience approximately 50 F–T cycles annually (Bartczak et al. 2022), while more severe alpine or high-altitude climates can exceed 100 cycles per year (Climate Atlas of Canada, 2022; Wang et al. 2024). In Hungary, building stones are typically subjected to 50–70 F–T cycles per year, with winter temperatures reaching –10 °C.

In this study, the mechanical degradation and microstructural evolution of 11 representative lithotypes from the Eger region were investigated. By exposing 468

specimens to these replicated environmental regimes and measuring ultrasonic wave velocities and bulk density, this research identifies the thresholds for fatigue-induced damage in Hungarian stones.

2. MATERIALS AND METHODS

2.1. Investigated materials and geological setting

The specimens were sourced from active and historical quarries in the vicinity of Eger, Northeastern Hungary (Bükk Mountains). The following materials are historically significant for the region's architectural heritage:

- Sandstones (S1–S5): These belong to the Pétervására Sandstone Formation (Lower Miocene). The suite ranges from fine-grained, well-sorted calcareous sandstones (S1, S2) to coarse-grained conglomeratic facies (S3, S4, S5). As shown in Figure 1, the coarser varieties are characterized by rounded lithic pebbles and ferruginous staining, indicating high-energy deposition.

Figure 1
Sandstone blocks used for sample preparation

- Volcanic Tuffs (T1–T6): These are Miocene Rhyolitic Tuffs. As illustrated in Figure 2, the samples show varying alteration: T2, T3, and T5 exhibit yellowish-ochre hues from zeolitization (clinoptilolite), T4 shows a greenish tint from celadonite alteration, and T6 is a pristine, pumice-rich vitric tuff. These rocks feature a highly connected pore network.

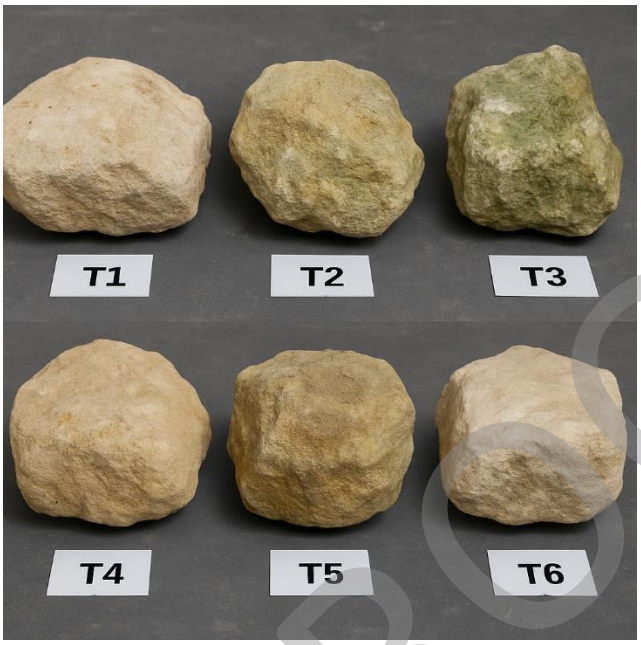

Figure 2
Rhyolite tuff blocks used for sample preparation

2.2. Experimental program and workflow

The investigation followed a systematic sequence to quantify physical degradation. Altogether, 468 specimens were fabricated using a high-precision diamond core drill. Two specific geometries were employed:

- Cylindrical specimens (diameter: 30 mm, height: 60 mm) were used for petrophysical and uniaxial compression tests.
- Disc specimens (diameter: 30 mm, height: 30 mm) were utilized for Brazilian tensile tests.

The testing sequence followed a consistent workflow: pre-conditioning → petrophysical characterization → post-test evaluation (Figure 3).

The results of these investigations allow for the quantification of damage thresholds, identifying the specific cycle at which internal micro-cracking leads to a critical reduction in the stones' stiffness and durability.

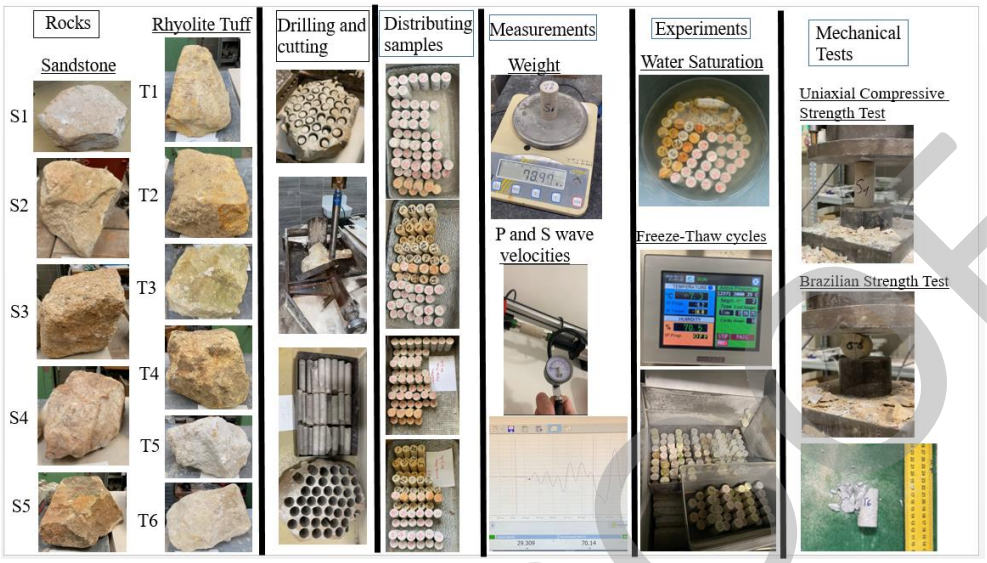

Figure 3

Experimental workflow: from sample preparation to petrophysical and mechanical characterization

2.3. Environmental exposure regimes

To replicate key environmental conditions, the program included four exposure regimes:

2.3.1. Air-Dry condition

The first group served as the baseline reference for all subsequent analyses. Specimens were placed in a controlled laboratory environment at a constant temperature of 22 ± 2 °C and relative humidity of approximately 45–55%. They were stored for at least Two weeks before testing to achieve moisture equilibrium and ensure all samples were in a stable, naturally dry state. This condition simulated stones exposed to moderate temperate climates, where temperature fluctuations are limited and the rocks remain relatively dry. The measurements obtained under this condition represent the intrinsic physical and mechanical characteristics of the materials before any environmental alteration.

2.3.2. Water-saturated condition

The second group assessed the effects of water absorption on the rocks' physical and mechanical properties. Specimens were fully immersed in deionized water at 22 ± 2 °C for 72 h in sealed containers, with mass recorded every 6 h; full saturation was assumed when mass changes fell below 0.1%. Saturated samples were removed, gently surface-dried, and weighed for density and porosity calculations. All petrophysical and dynamic tests were performed within 30 minutes, measuring:

1. Bulk density (ρ): mass per unit volume, indicating porosity and compactness.
2. P-wave velocity (V_p): speed of compressional waves, reflecting stiffness and continuity.
3. S-wave velocity (V_s): speed of shear waves, indicating shear stiffness.
4. Dynamic elastic parameters (from ρ, V_p, V_s):
    - Dynamic Young's modulus (E_{dyn}): stiffness under stress.
    - Shear modulus (G_{dyn}): resistance to shape changes under shear.
    - Bulk modulus (K_{dyn}): resistance to uniform compression.
    - Poisson's ratio (ν_{dyn}): lateral expansion under vertical compression, indicating ductility and microcrack structure.

2.3.3. Freeze–Thaw cycling (50 and 100 cycles)

The third and fourth groups assessed the effects of cyclic freezing and thawing on sandstone and tuff durability, considering the influence of mineral composition and porosity on freeze–thaw resistance (Moghrabi et al. 2025b). Experiments simulated Central European and high-altitude continental climates using a fully automated freeze–thaw chamber alternating between −10 °C and +25 °C with 80–95 % relative humidity. Each 12-hour cycle included 6 h of freezing and 6 h of thawing. Specimens underwent 50 cycles (~25 days) or 100 cycles (~50 days), remaining in the chamber between cycles to prevent uncontrolled drying. After the final cycle, samples were surface-dried, stabilized for 30 min at 22 ± 2 °C, and tested following the procedures described in Section 2.2 to quantify changes in petrophysical properties.

3. RESULTS

3.1. Acoustic impedance

Acoustic impedance is a material property that quantifies the resistance of a medium to the propagation of compressional (P-) waves. It is calculated as the product of the material's bulk density (ρ) and the P-wave velocity (V_p). The velocity was calculated using the travel time (t) and the sample length (L) as follows $V_p = \frac{L}{t}$. Consequently, the acoustic impedance is expressed as:

$$Z = \rho * Vp \quad (1)$$

Table 1 presents the variation in acoustic impedance of tuff and sandstone specimens subjected to different environmental conditions, highlighting clear lithological and durability-related contrasts. For tuff, the average acoustic impedance increased from 2.94 ×10⁶ kg/(m²·s) in the dry state to 3.66 ×10⁶ kg/(m²·s) under water saturation, reflecting the strong influence of pore filling on wave transmission in this highly porous rock.

The subsequent reduction to 3.32 ×10⁶ kg/(m²·s) after 50 freeze–thaw cycles and further to 2.98 ×10⁶ kg/(m²·s) after 100 cycles indicates progressive internal damage,

associated with pore expansion, microcrack development, and partial loss of matrix continuity.

Table1

Acoustic impedance of tuff and sandstone under different environmental conditions

Rocks		Normal Dry	Water Saturation	Freeze-thaw 50 cycles	F-T 100 cycles
		Acoustic impedance *10^6 (kg.m^{-2}.s^{-1})			
Tuff	**T1**	2.99	3.95	3.33	2.72
	T2	3.41	4.05	3.61	3.34
	T3	2.48	3.34	2.82	2.68
	T4	3.83	4.24	4.14	3.89
	T5	2.33	3.02	2.83	2.7
	T6	2.61	3.38	3.20	2.52
	Average	2.94	3.66	3.32	2.98
Sandstone	**S1**	7.01	7.10	6.56	6.19
	S2	4.18	4.69	4.43	4.39
	S3	6.12	7.54	6.42	6.04
	S4	5.31	5.69	5.56	5.18
	S5	6.49	6.83	6.44	6.06
	Average	5.82	6.37	5.88	5.57

Individual tuff samples show noticeable scatter, confirming the heterogeneity of the rock fabric and varying sensitivity to frost action. In contrast, sandstone exhibits significantly higher acoustic impedance values, with an average increase from 5.82 $\times 10^6$ kg/(m²·s) in dry conditions to 6.37 $\times 10^6$ kg/(m²·s) upon saturation, suggesting improved elastic wave coupling due to water-filled microvoids without structural weakening.

Although freeze–thaw cycling leads to a gradual decrease to 5.88 $\times$ 10^6 and 5.57 $\times 10^6$ kg/(m²s) after 50 and 100 cycles, respectively, the reduction is relatively moderate, indicating limited crack growth and preservation of grain interlocking. Overall, the results demonstrate that acoustic impedance is highly sensitive to environmental conditions and effectively captures stiffness degradation, with tuff showing pronounced vulnerability to freeze–thaw damage, while sandstone maintains greater mechanical stability due to its denser and more competent microstructure.

3.2. Dynamic Young's modulus (E_{dyn})

Figure 4 illustrates the changes in dynamic Young's modulus (E_{dyn}) of sandstone and tuff under varying environmental states. Dynamic Young's modulus represents the elastic stiffness of a material under small, dynamic strains and is derived from

ultrasonic P-wave and S-wave velocities along with bulk density, making it a sensitive, non-destructive indicator of rock stiffness and internal integrity.

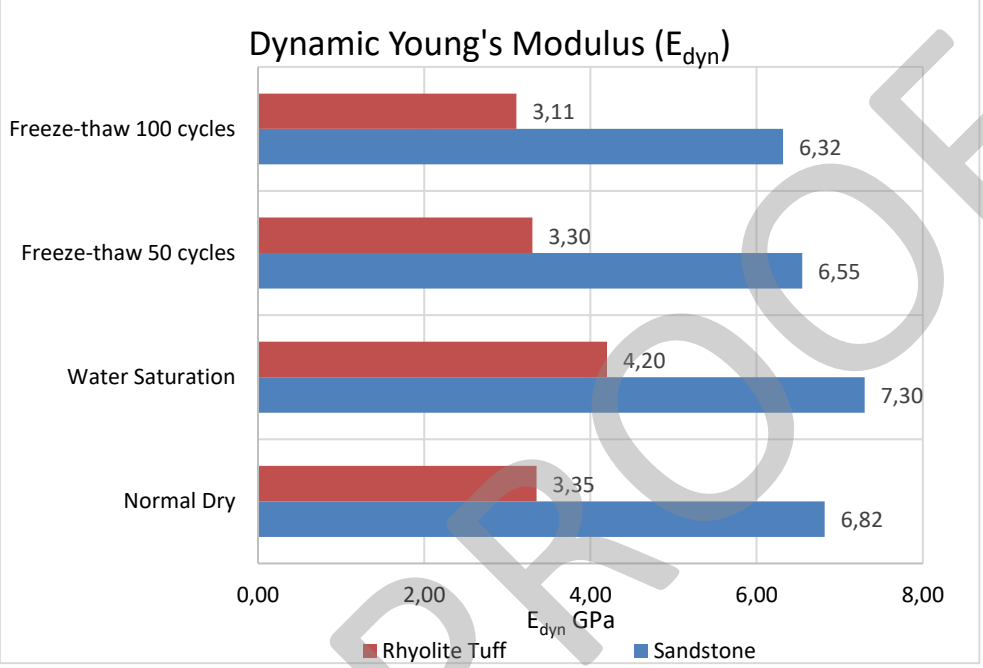

Figure 4

Variation of dynamic Young's modulus (E_{dyn}) of tuff and sandstone under different environmental conditions

The results highlight clear differences in stiffness and durability between the two lithotypes. In sandstone, E_{dyn} increased from 6.82 GPa in the dry state to 7.30 GPa under water saturation, indicating enhanced elastic stiffness due to pore filling and improved stress wave transmission through the rock framework. This increase suggests that saturation improves contact efficiency between mineral grains without causing structural weakening in the dense and well-cemented sandstone matrix.

With the application of freeze–thaw cycles, sandstone exhibited a gradual reduction in dynamic modulus to 6.55 GPa after 50 cycles and 6.32 GPa after 100 cycles. This moderate decrease reflects limited microcrack initiation and slow degradation of intergranular bonding, confirming the rock's relatively high resistance to cyclic freezing and thawing. The retained stiffness indicates that the primary load-bearing skeleton of sandstone remains largely intact despite repeated thermal stress.

In contrast, tuff showed significantly lower E_{dyn} values under all conditions, increasing from 3.35 GPa in the dry state to 4.20 GPa upon saturation, followed by a continuous decline to 3.30 GPa and 3.11 GPa after 50 and 100 freeze–thaw cycles, respectively. This behavior highlights the strong influence of porosity and weak

bonding on the mechanical response of tuff, while water initially enhances stiffness through the pore-filling effect, freeze–thaw action rapidly promotes microcrack growth, pore expansion, and loss of elastic integrity. Overall, the results demonstrate that dynamic Young's modulus is highly sensitive to environmental degradation, with sandstone maintaining higher stiffness and durability, while tuff exhibits pronounced susceptibility to F-T induced mechanical weakening.

3.3. Dynamic Poisson's ratio (ν_{dyn})

Figure 5 presents the changes in dynamic Poisson's ratio (ν_{dyn}) of sandstone and tuff under different environmental conditions. Dynamic Poisson's ratio describes the relationship between lateral and axial strain under dynamic loading and is calculated from ultrasonic P- and S-wave velocities. It serves as a sensitive parameter for assessing deformation behavior and the evolution of microstructural damage in rock materials.

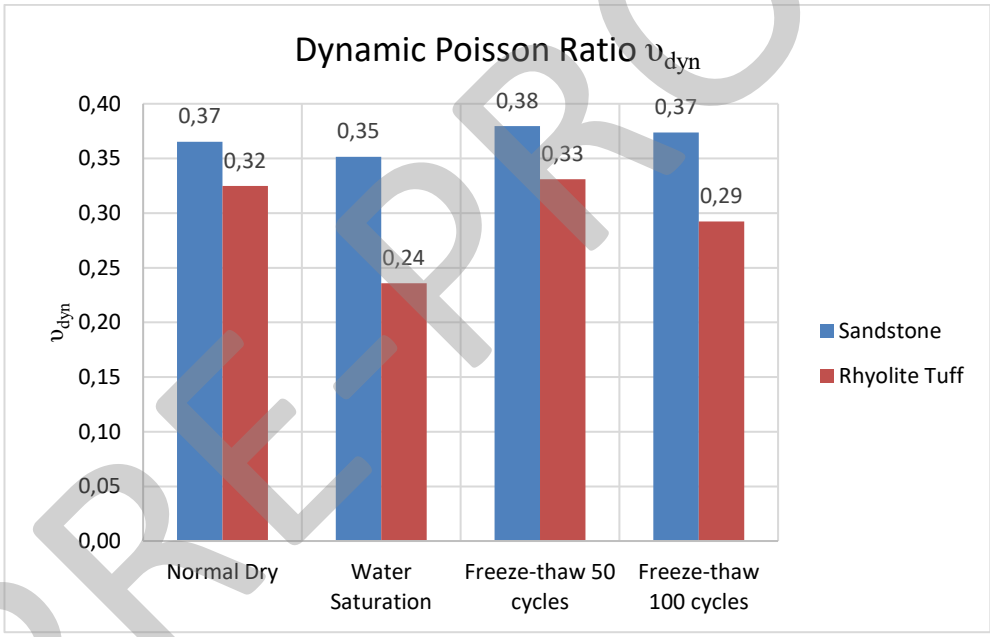

Figure 5
Variation of dynamic Poisson's ratio (ν_{dyn}) of tuff and sandstone under different environmental conditions

The results reveal differences in lateral deformation and damage evolution between sandstone and tuff. In sandstone, ν_{dyn} decreased slightly from 0.37 (dry) to 0.35 under water saturation, indicating stabilized elastic behavior, and rose to 0.38 after 50 freeze–thaw cycles before returning to 0.37 after 100 cycles, reflecting limited microcrack development and preservation of the load-bearing framework. Tuff exhibited lower ν_{dyn} values and greater sensitivity, dropping from 0.32 (dry) to

0.24 when saturated, then increasing to 0.33 after 50 cycles and decreasing to 0.29 after 100 cycles, highlighting the onset of microcrack growth and a reduction in elastic continuity. Overall, the dynamic Poisson's ratio effectively captures the internal stiffness redistribution and environmental degradation in both rocks, confirming that the tuff is significantly more susceptible to fatigue than the sandstone.

3.4. Dynamic Shear modulus (G_{dyn})

Based on Figure 6, sandstone consistently exhibits a higher dynamic shear modulus (G_{dyn}) than tuff under all environmental conditions. Dynamic shear modulus represents the material's resistance to shear deformation under small, dynamic strains and is derived from ultrasonic shear-wave velocity and bulk density, making it a reliable indicator of the integrity and stiffness of the rock framework.

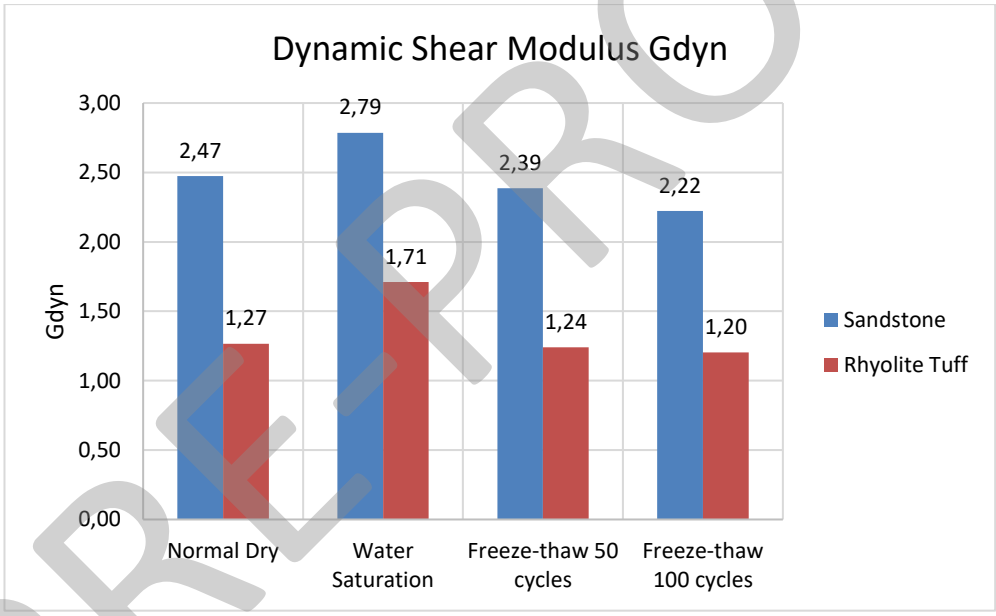

Figure 6
Variation of Dynamic Shear Modulus (G_{dyn}) for Sandstone and Tuff under Different Environmental Conditions

The higher G_{dyn} values observed in sandstone indicate a stiffer and mechanically stronger rock fabric, which is expected given sandstone's denser grain packing and stronger intergranular cementation compared to the more porous and heterogeneous structure of tuff.

Under normal dry conditions, the average G_{dyn} of sandstone (2.47 GPa) is almost double that of tuff (1.27 GPa), clearly reflecting the fundamental lithological differences between the Two rock types. When water saturation is introduced, both

rocks show an increase in dynamic shear modulus, with tuff increasing to 1.71 GPa and sandstone to 2.79 GPa; this behavior is typical in dynamic measurements, as water filling pores and microcracks enhances wave transmission and reduces energy loss, giving an apparent increase in stiffness, an effect that is more pronounced in tuff due to its higher porosity and greater sensitivity to pore-fluid interaction.

The freeze–thaw process causes a significant reduction in rigidity for both rock types, particularly after 50 cycles, which marks the onset of substantial microstructural damage. The average G_{dyn} of tuff drops sharply from 1.71 GPa in the saturated state to 1.24 GPa after 50 cycles, while sandstone decreases from 2.79 GPa to 2.39 GPa, indicating that ice crystallization within pores and pre-existing flaws leads to microcrack initiation and propagation. The larger reduction observed in tuff highlights its weaker cementation and larger pore spaces, which allow more extensive ice expansion and internal stress development, making it mechanically less durable under cyclic freezing conditions. Sandstone, although affected, retains a higher proportion of its stiffness due to its more compact texture and stronger grain bonding.

After 100 freeze–thaw cycles, the rate of degradation decreases for both rocks, with tuff showing only a slight further reduction to 1.20 GPa and sandstone decreasing to 2.22 GPa, suggesting that most structural damage occurs during the early stages of freeze–thaw exposure. This behavior indicates a damage saturation effect, where initial cycles create most microcracks, and subsequent cycles mainly widen or reactivate existing discontinuities rather than generating new ones. These trends imply that tuff is highly sensitive to environmental conditions involving moisture and temperature fluctuations and may pose durability concerns in cold or water-rich environments, whereas sandstone demonstrates better mechanical stability and long-term performance despite still experiencing progressive stiffness degradation under severe freeze–thaw action.

3.5. Dynamic Bulk modulus (K_{dyn})

According to Figure 7, the average dynamic bulk modulus (K_{dyn}) clearly shows that sandstone is significantly stiffer than tuff under all environmental conditions. Dynamic bulk modulus represents the resistance of a rock to uniform volumetric compression under dynamic loading and is derived from ultrasonic P- and S-wave velocities together with bulk density, making it a sensitive indicator of volumetric stiffness and compressibility of the rock mass. The higher K_{dyn} values indicate a much lower volumetric deformability and a stronger resistance to compression in sandstone.

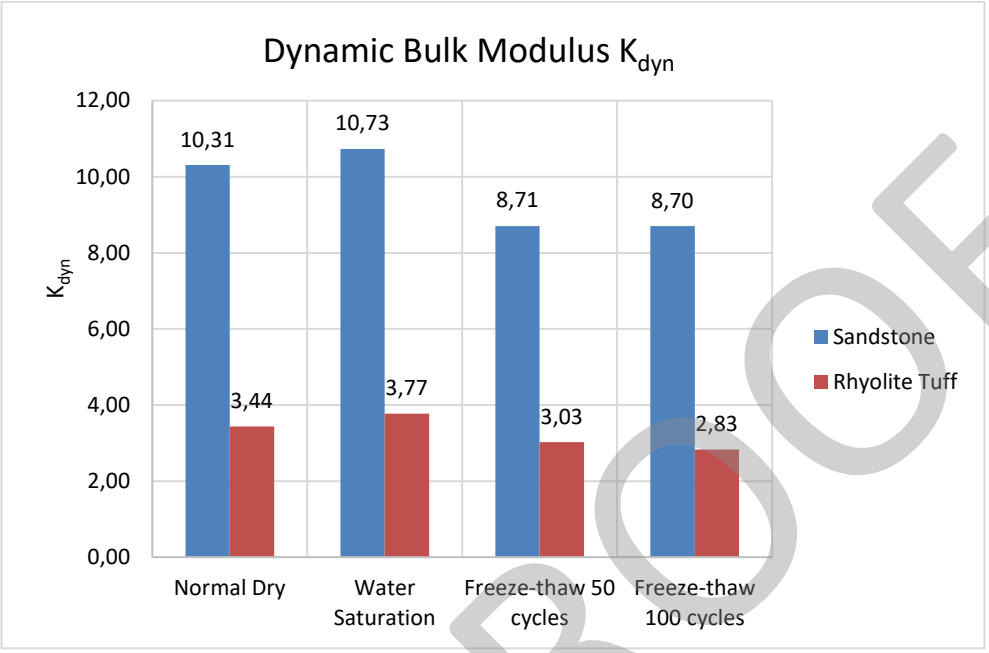

Figure 7

Variation of Dynamic Bulk Modulus (K_{dyn}) for Sandstone and Tuff under Different Environmental Conditions

Under dry conditions, sandstone has an average K_{dyn} of 10.31 GPa, nearly three times higher than tuff (3.44 GPa) due to its denser grain framework and stronger cementation. Water saturation slightly increases K_{dyn} for both rocks (10.73 GPa for sandstone, 3.77 GPa for tuff) by reducing compressibility, an effect more pronounced in tuff. Freeze–thaw cycles reduce volumetric stiffness, with K_{dyn} dropping to 8.71 GPa (sandstone) and 3.03 GPa (tuff) after 50 cycles, reflecting microcrack growth, while further cycling to 100 cycles causes minimal additional decrease (8.70 GPa and 2.83 GPa). These results highlight tuff's high environmental sensitivity and sandstone's superior durability under moisture and freeze–thaw conditions.

3.6. Correlations

3.6.1. Correlation between G_{dyn} and Vs

Figure 9 illustrates the fundamental physical relationship in rock mechanics where the dynamic shear modulus (G_{dyn}) is directly proportional to the square of the ultrasonic shear wave velocity (V_s), modified by the material's bulk density (ρ). This relationship is defined by the elastic wave theory equation:

$$G_{dyn} = \rho * Vs^2 \quad (2)$$

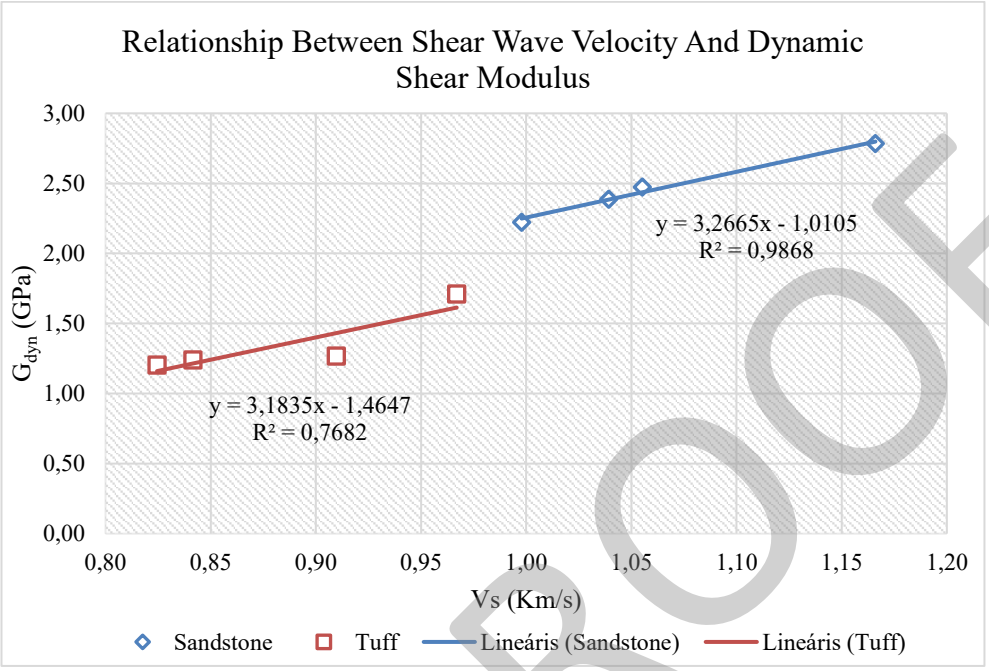

Figure 8

Correlation between Dynamic Shear Modulus (G_{dyn}) and Ultrasonic wave velocity (Vs) for Sandstone and Tuff rocks

This strong correlation is expected because G_{dyn} is a measure of a rock's intrinsic stiffness and resistance to shear deformation, while Vs measures how efficiently shear stress waves propagate through that stiff framework. The wave velocity is fundamentally governed by the rock's internal physical parameters, primarily its density and its porosity, as well as the stiffness of the grain contacts, cementation, and the presence of microcracks or saturation. Higher density and lower porosity generally result in higher wave velocities and greater stiffness.

The data clearly indicates that the sandstone is a significantly stiffer material than the tuff under dynamic (small strain) conditions, showing much higher G_{dyn} values for comparable V_s measurements. This difference in mechanical behavior stems from internal rock properties; the sandstone likely possesses a lower overall porosity, better-cemented grain contacts, or a different grain size distribution compared to the tuff. The high coefficient of determination for sandstone (R^2 = 0.9868) suggests a very consistent, homogeneous material response, while the lower value for tuff (R^2=0.7682) indicates greater variability in its internal structure, possibly higher or more variable porosity, or more microcracks.

Analyzing the linear regression equations themselves provides further insight. The sandstone equation is y=3.2665x−1.0105, and the tuff is y=3.1835x−1.4647. The slopes are relatively similar, indicating a comparable rate of increase in Gdyn per unit increase in V_s, but the difference in intercepts highlights the overall offset in

stiffness. The higher negative intercept for tuff corresponds to its lower overall Gdyn values for the same V_s range, quantitatively confirming its reduced stiffness compared to the sandstone. The high R-squared values confirm that for both materials, ultrasonic shear wave velocity is a reliable predictor for the dynamic shear modulus.

3.6.2. Correlation between E_{dyn} and Vp

Figure 9 illustrates the change in the dynamic Young's modulus as a function of the P-wave velocity. The sandstone exhibits a higher correlation (R^2 = 0.9213) compared to the tuff (R^2 = 0.856) across the range from the normal dry state to the 100th freeze–thaw cycle.

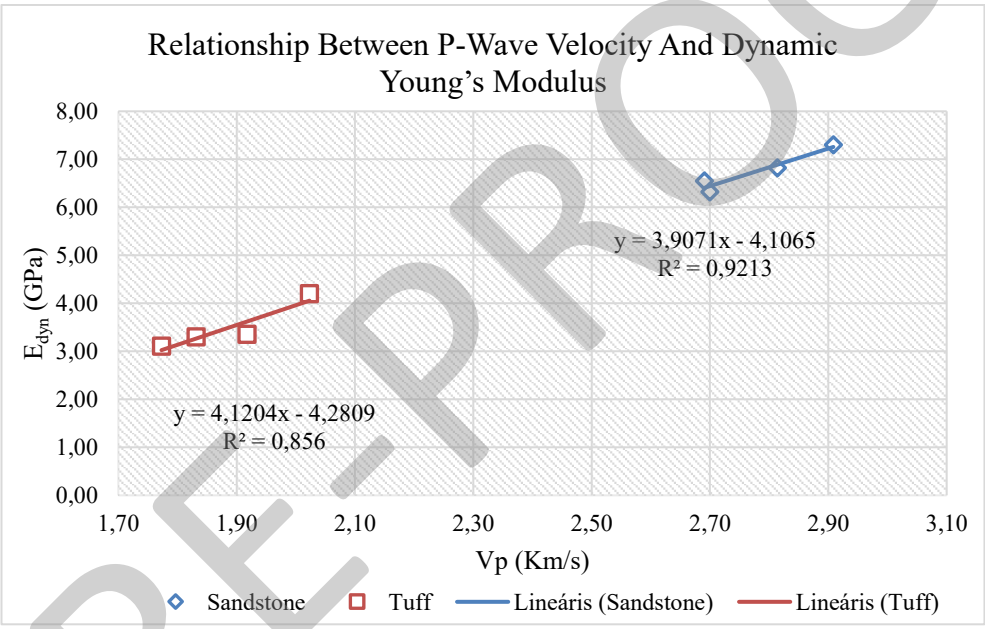

Figure 9
Correlation between Dynamic Young Modulus E_{dyn} and Ultrasonic wave velocity (V_p) for Sandstone and Tuff rocks

It means that the observed correlations originate from the fundamental physical link between E_{dyn} and V_p, since both parameters are governed by the elastic stiffness, density, and integrity of the rock's microstructure. In elastic wave theory, P-wave velocity directly depends on Young's modulus and bulk stiffness, meaning that any change in crack density, pore structure, or grain contact stiffness simultaneously affects both values. For sandstone, the very high correlation (R^2 = 0.9213) indicates that this theoretical relationship is well preserved from normal dry conditions through 100 freeze–thaw cycles, reflecting a relatively homogeneous fabric where microcrack development occurs in a consistent and progressive manner. As damage

accumulates, reductions in wave velocity are directly mirrored by proportional reductions in dynamic Young's modulus, confirming that ultrasonic measurements reliably capture stiffness degradation in sandstone.

For tuff, although the correlation remains strong (R^2 = 0.856), it is noticeably lower due to its more complex and heterogeneous internal structure. The higher porosity, variable pore geometry, and weaker bonding in tuff lead to non-uniform crack initiation and localized damage during saturation and freeze–thaw cycling, causing greater scatter in the relationship between V_p and E_{dyn}. While both parameters are still controlled by the same elastic framework, additional mechanisms such as pore collapse, crack coalescence, and fluid–solid interactions reduce the linearity of their relationship.

4. DISCUSSION AND CONCLUSIONS

4.1. Discussion

The results demonstrate that water saturation and freeze–thaw (F-T) cycling exert a systematic influence on the petrophysical and dynamic elastic properties of both lithologies, though sandstone consistently exhibits higher stability and smaller relative variations than tuff. Water saturation initially increases density, ultrasonic velocities (V_p, V_s), and dynamic moduli (E_{dyn}, G_{dyn}, K_{dyn}) in both rocks. This transient "stiffening" reflects the filling of pore spaces with water, which enhances wave transmission and reduces internal scattering. The effect is significantly more pronounced in tuff due to its higher porosity and pore connectivity; however, this represents a change in wave propagation conditions rather than a gain in load-bearing capacity.

The application of F-T cycles induces progressive degradation in all dynamic parameters, with the most significant damage occurring within the first 50 cycles. This confirms that early F-T exposure is critical for microstructural damage development, as ice expansion generates internal stresses that propagate microcracks and reduce grain-to-grain contact efficiency. Tuff is particularly vulnerable, showing marked declines in acoustic impedance and elastic moduli. In contrast, sandstone retains a larger proportion of its original stiffness, confirming a more resilient fabric and higher resistance to frost-induced deterioration.

A damage saturation effect was observed after 100 F-T cycles, where the rate of degradation stabilized for both lithologies. Once a critical microcrack network is established during early cycles, subsequent freezing events primarily propagate existing defects rather than initiating new ones. This stabilization is particularly evident in the dynamic shear and bulk moduli, where changes beyond 50 cycles remain minor. While the primary load-bearing framework of sandstone remains largely intact, the heterogeneous and weakly bonded matrix of the tuff continues to exhibit greater variability in its elastic response.

Strong correlations between ultrasonic wave velocities and dynamic moduli (E_{dyn}-V_p and G_{dyn}-V_s) confirm that non-destructive ultrasonic testing is a reliable tool for monitoring environmental degradation. Sandstone exhibited higher coefficient of

determination (R^2), indicating that stiffness changes are directly and uniformly reflected in wave propagation. The slightly higher scatter observed in tuff results from internal heterogeneity and non-uniform crack development. Ultimately, this integrated analysis of petrophysical and dynamic parameters provides a coherent framework for quantifying durability and damage evolution in building stones under cyclic environmental stress.

4.2. Conclusions

This study identifies critical fatigue thresholds and mechanical responses of Hungarian sandstone and tuff under cyclic environmental stress. Based on the findings, the following conclusions are drawn:

- Environmental Sensitivity and Lithological Control: The degree of physical degradation is primarily governed by the interaction between lithology and pore geometry. While water saturation provides a transient increase in wave transmission through pore-filling effects, it simultaneously creates the hydraulic conditions necessary for frost-heaving.
- Damage Kinetic Thresholds: Microstructural damage is not linear. A critical fatigue threshold exists within the first 50 freeze–thaw cycles, where most of the microcrack initiation and pore expansion occurs. Beyond this threshold, the rate of degradation diminishes, suggesting a damage saturation effect where subsequent cycles primarily reactivate existing discontinuities rather than generating new ones.
- Contrast in Volumetric Stiffness: Sandstone maintains superior structural integrity due to its competent grain-to-grain interlocking, whereas volcanic tuff is highly susceptible to zeolitic alteration and pore-linkage. The significant loss in dynamic shear and bulk moduli in tuff highlights a rapid loss of resistance to volumetric compression.
- Predictive Value of Non-Destructive Testing: Strong correlations between acoustic impedance and dynamic elastic parameters confirm that ultrasonic wave velocities serve as a reliable, non-destructive proxy for quantifying internal damage and predicting the long-term durability of these lithotypes in temperate climates.

REFERENCES

Altındag, R. (2012). Investigation of some correlations between p-wave velocity and some mechanical properties for sedimentary rocks. *Journal of the Southern African Institute of Mining and Metallurgy*, 112 (3), pp. 229–237.

Arman, H., Aydin, M., Karaman, K. (2020). Correlating natural, dry, and saturated ultrasonic pulse velocities with the mechanical properties of rock for various

sample diameters. *Applied Sciences*, 10 (24), 9134, https://doi.org/10.3390/app10249134.

Bartczak, A., Piotrowski, P., Czarnecka, M. (2022). Freeze–thaw cycles in poland in the period 1951–2018. *Theoretical and Applied Climatology*, 149, pp. 1171–1185, https://doi.org/10.1007/s00704-022-04002-7.

Climate variables: freeze–thaw days. [Online]. Available: https://climateatlas.ca, (last accessed 23 April 2026).

de Gennaro, M., Cappelletti, P., Langella, A., Mercurio, M., Scarpati, C. (2000). Building stones of naples: the neapolitan yellow tuff and its physical–mechanical properties. *Engineering Geology*, 57 (1–2), pp. 1–14.

Galaura, G., Evangelista, L., Siringan, F. (2019). Geotechnical characterization of the diliman tuff in metro manila, philippines. *Geotechnical and Geological Engineering*, 37 (3), pp. 1863–1877, https://doi.org/10.1007/s10706-018-0690-8.

Jia, H., Ding, S., Zi, F., Dong, Y., Shen, Y. (2020). Evolution in sandstone pore structures with freeze-thaw cycling and interpretation of damage mechanisms in saturated porous rocks. *Catena*, 195, 104915, https://doi.org/10.1016/j.catena.2020.104915.

Kahraman, S. (2001). Evaluation of simple methods for assessing the uniaxial compressive strength of rock. *International Journal of Rock Mechanics and Mining Sciences*, 38 (7), pp. 981–994.

Ma, J., Jin, J., Li, W. (2023). Study on the pore structure characteristics and damage constitutive model of sandstone under freeze-thaw conditions. *Frontiers in Earth Science*, 11, 1095686, https://doi.org/10.3389/feart.2023.1095686.

Moghrabi, R., Török, Á., Vásárhelyi, B. (2025a). Comparative study of physical and mechanical properties of limestone and sandstone at varying temperature condition. *Rock Mechanics Letters*, 2, pp. 189–194, https://doi.org/10.70425/rml.202504.25.

Moghrabi, R., Török, Á., Vásárhelyi, B. (2025b). Impact of low temperature, saturation, and freeze-thaw cycles on the mechanical and physical properties of tuff and sandstone rocks. *RockEng2025, Montreal, Canada*, 24–27 August 2025.

Niu, Y., Li, G., Wang, Y., Zhang, M. (2024). Pore structure expansion and evolution in sandstone with prefabricated crack under freeze-thaw cycles based on ct

scanning. *Frontiers in Earth Science*, 12, 1394731, https://doi.org/10.3389/feart.2024.1394731.

PAGASA: climate of the philippines. [Online]. Available: https://bagong.pagasa.dost.gov.ph, (last accessed 23 April 2026).

Putnis, A., Mauthe, G. (2000). The effect of pore size on cementation in porous rocks. *Geofluids*, 1 (1), pp. 37–41.

Rodriguez-Navarro, C., Doehne, E. (1999). Salt weathering: influence of evaporation rate, supersaturation and crystallization pattern. *Earth Surface Processes and Landforms*, 24 (3), pp. 191–209.

Ruedrich, J., Bartelsen, T., Siegesmund, S. (2011). Moisture expansion as a deterioration factor for sandstone used in buildings. *Environmental Earth Sciences*, 63, pp. 1545–1564.

Scherer, G. W. (2004). Stress from crystallization of salt. *Cement and Concrete Research*, 34 (9), pp. 1613–1624.

Siegesmund, S., Gross, C. J., Dohrmann, R., et al. (2023). Moisture expansion of tuff stones and sandstones. *Environmental Earth Sciences*, 82, 146.

Wang, X., Chen, Z., Zhou, Y., Li, J. (2024). Spatial distribution and frequency of freeze–thaw cycles on the qinghai–tibet plateau and its implications for engineering stability. *Engineering Geology*, 330, 107087, https://doi.org/10.1016/j.enggeo.2024.107087.

Zhang, J., Gao, F., Li, J., Zhou, K., Yang, C. (2025). Pore structure evolution characteristics and damage mechanism of sandstone subjected to freeze–thaw cycle treatment. *Fractal and Fractional*, 9 (5), 293.

Zhou, K., Yang, C., Zhang, J., Li, B. (2025). Experimental study on damage characteristics of sandstone under freeze-thaw actions: insights into pore structure evolution and hydraulic connectivity. *Theoretical and Applied Fracture Mechanics*, 135, 104782.